

Crystal Structures and Luminescence Properties of Pd(II) and Pt(II) Complexes with 2,5-Bis(thiophene)-1-nonyl-3,4-bis(methylthio)pyrrole

Jun-Gill Kang,* Sung-Il Oh, Dong-Hee Cho, Min-Kook Nah, Changmoon Park, Young Ju Bae,[†]
Woo Tack Han,[†] Young Jin Park,[†] Sang Woo Lee,[†] and In Tae Kim^{†,*}

Department of Chemistry, Chungnam National University, Daejeon 305-764, Korea. *E-mail: jgkang@cnu.ac.kr

[†]Department of Chemistry, Kwangwoon University, Seoul 139-701, Korea. *E-mail: itkim@kw.ac.kr

Received February 6, 2009, Accepted March 26, 2009

Complexes of Pd(btnbmtp)Cl₂ and Pt(btnbmtp)Cl₂ (btnbmtp = 2,5-bis(thiophen)-1-nonyl-3,4-bis(methylthio)-pyrrole) were prepared and their crystal structures were determined at room temperature. In the structures, the two thiophene moieties lie in cis form with an average dihedral angle of 55.26° to the pyrrole frame. The luminescence properties of the free ligand and the complexes were investigated in solution and solid states. The luminescence of the compounds were not favored by substituting thiophene moieties to the pyrrole frame, compared to the unsubstituted nbmtp (nbmtp = 1-nonyl-3,4-bis(methylthio)pyrrole). In particular, thiophene substitution quenched the emission from the complexes dissolved in CH₂Cl₂ and reduced the charge transfer transitions from S atoms of the thio moieties to Pt in crystalline state, which was very characteristic of Pt(nbmtp)Cl₂.

Key Words: 2,5-Bis(thiophen)-1-nonyl-3,4-bis(methylthio)pyrrole, Pt(II), Pd(II), X-ray structure, Luminescence

Introduction

The design and synthesis of conducting polymers such as polypyrrole and polythiophene have attracted a great deal of attention due to their possible applications to electrochromic-devices,¹ electrochemical cell,² light-emitting diodes,³ and energy storage device.⁴ Furthermore, the addition of a functional group at the 3- and 3,4-positions of pyrrole and thiophene plays an important role in solubility, conductivity and morphology of their corresponding polymers.^{5,6} Recently, Meijer and co-workers synthesized 3,4-bis(alkylthio)thiophene and its polymer, and investigated the optical and electrochemical properties of these thiophen derivatives upon the complexation toward transition metal ions.^{7,8} Complexation diminishes the electron-donor ability of the sulfur to the thiophen ring and quenches the fluorescence of the derivatives. Recently, we reported the synthesis and structural and optical properties of Pd(II) and Pt(II) complexes with 1-nonyl-3,4-bis(methylthio)pyrrole (nbmtpH₂).^{9,10} It was found that the complex of Pt(nbmtp)Cl₂ produced emission at 618 nm via a charge transfer from S to Pt(II) in main and from the pyrrole ring to Pt(II) in minor. In this study, we synthesized 2,5-bis(thiophen)-1-nonyl-3,4-bis(methylthio)pyrrole (btnbmtpH₂) in which thiophenes were substituted at the 2 and 5 positions of nbmtpH₂ and investigated the substitution effect on the optical properties of Pd(II) and Pt(II) complexes with btnbmtp and Cl. The new compounds will also be applied to be for Sonogashia reaction¹¹ as Pd and Pt catalyst and organic light-emitting diodes (OLEDs) as emitting materials.

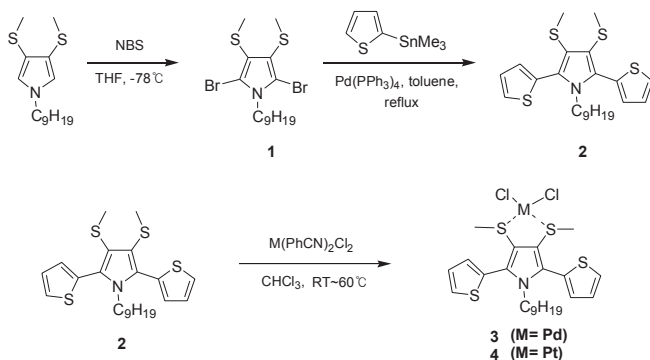
Experimental

Synthesis. 2,5-Dibromo-1-nonyl-3,4-bis(methylthio)pyrrole (1): A solution of nbmtpH₂ (2.87 g, 10.0 mmol) was prepared in 115 mL of dried THF at -78 °C under nitrogen atmosphere.

To this solution was added 3.57 g of *N*-bromosuccinide dissolved in 90 mL of THF. The mixture was stirred for 12 h at room temperature, the solvent was removed *in vacuo*, and the crude product was purified by column chromatographic purification on silica gel with hexane and CH₂Cl₂ (19:1) to afford 4.0 g (90.2%) of the title compound as a yellow liquid. ¹H NMR (400 MHz, CDCl₃) δ 3.95-3.91 (t, 2H), 2.2 (s, 6H), 1.62-1.59 (m, 2H), 1.25-1.18 (m, 12H), 0.80-0.77 (t, 3H); ¹³C NMR (100 MHz, CDCl₃) δ 119.5, 108.8, 49.1, 31.6, 29.7, 29.1, 28.99, 28.91, 26.2, 22.4, 19.6, 13.9; GC-MS (rel.intensity) 443 (M⁺, 54), 317 (12), 283 (100), 252 (33), 236 (21), 212 (43), 198 (22), 171 (9.3); IR (KBr) ν_{max} 2960, 2925, 2854, 2733, 1739, 1457, 1434, 1371, 1336, 1269, 1129, 1082, 972 cm⁻¹; Abs. λ_{max} (in CH₂Cl₂ solution) 237.8 nm.

BtnbmtpH₂(2): A solution of tributyl(2-thienyl)tin (0.555 g, 1.488 mmol), **1** (0.3 g, 0.67 mmol), and tetrakis(triphenylphosphine) palladium(0) (0.039 g, 0.0338 mmol) in toluene (10 mL) was heated at reflux for 18 h under a nitrogen atmosphere. The mixture was concentrated *in vacuo* and subjected to column chromatography on silica gel with hexane and CH₂Cl₂ (19:1) to afford 0.26 g (86.7 %) of the title compound as a yellow liquid. ¹H NMR (400 MHz, CDCl₃) δ 7.48-7.47 (m, 2H), 7.167.13 (m, 4H), 3.87-3.83 (t, 2H), 2.27 (s, 6H), 1.441.39 (m, 2H), 1.25-0.92 (m, 12H), 0.88-0.84 (t, 3H); ¹³C NMR (100 MHz, CDCl₃) δ 131.8, 130.1, 129.4, 127.3, 126.9, 119.6, 46.0, 31.7, 30.9, 29.1, 29.0, 28.6, 26.2, 22.6, 20.8, 14.1; IR (KBr) ν_{max} 3105, 3070, 2956, 2921, 2854, 1653, 1559, 1457, 1418, 1367, 1297, 1223, 1187, 1078, 1046, 969, 850, 834, 698; Abs. λ_{max} (in CH₂Cl₂ solution) 238.9 nm and 286 nm.

[Pd(btnbmtp)Cl₂](3) : 2 (0.26 g, 0.578 mmol) was added to a solution of [PdCl₂(PhCN)₂] (0.22 g, 0.578 mmol) in dry dichloromethane (16 mL). After stirring at room temperature for 20 min, the solvent was removed *in vacuo* and hexane was added to give a red precipitate of **(3)**, which was filtered off and dried *in vacuo* with a yield of 63.5 % (0.23 g) (see Scheme



Scheme 1

1). ^1H NMR (400 MHz, CDCl_3) δ 7.61–7.59 (m, 2H), 7.24–7.20 (m, 4H), 4.05–3.80 (m, 2H), 2.65–2.60 (d, 6H), 1.61–1.49 (m, 2H), 1.25–1.03 (m, 12H), 0.88–0.84 (t, 3H); ^{13}C NMR (100 MHz, CDCl_3) δ 130.4, 129.4, 129.4, 128.1, 127.2, 127.2, 126.6, 31.7, 31.0, 30.9, 29.0, 28.5, 28.5, 28.2, 27.7, 26.2, 22.5, 14.0; IR (KBr) ν_{max} 3081, 3015, 2925, 2854, 1653, 1559, 1417, 1230, 974, 849, 706; Abs. λ_{max} (in CH_2Cl_2 solution) 244.7 nm; Anal. Calcd for $\text{C}_{22}\text{H}_{29}\text{Cl}_2\text{NPdS}_4$: C, 43.10; H, 4.77; N, 2.28; S, 20.92. Found: C, 42.45; H, 4.02; N, 2.97; S, 20.82.

[Pt(btnbmtmp)Cl₂](4) (0.19 g, 0.423 mmol) was added to a solution of [PtCl₂(PhCN)₂] (0.2 g, 0.423 mmol) in dry chloroform (10 mL). After stirring at 60 °C for 6 h, the solvent was removed *in vacuo* and subjected to column chromatography on silica gel with hexane and ethyl acetate (30:1). The yellow precipitate was recrystallized with ethyl acetate to afford 0.09 g (30.3%) of the title compound as a yellow solid (see Scheme 1). ^1H NMR (400 MHz, CDCl_3) δ 7.61–7.60 (m, 2H), 7.26–7.22 (m, 4H), 4.05–3.80 (m, 2H), 2.67–2.62 (d, 6H), 1.58–1.50 (m, 2H), 1.25–1.04 (m, 12H), 0.88–0.84 (t, 3H); ^{13}C NMR (100 MHz, CDCl_3) δ 130.4, 130.4, 129.4, 129.3, 128.1, 127.5, 127.5, 47.3, 31.7, 31.0, 29.0, 29.0, 28.7, 28.6, 28.2, 26.2, 26.1, 22.5, 14.0; IR (KBr) ν_{max} 3077, 2955, 2924, 2853, 1739, 1461, 1414, 1375, 1234, 972, 707; Abs. λ_{max} (in CHCl_3 solution) 244.7 nm and 293.9 nm; Anal. Calcd for $\text{C}_{22}\text{H}_{29}\text{Cl}_2\text{NPtS}_4$: C, 37.66; H, 4.17; N, 2.00; S, 18.28. Found: C, 37.81; H, 4.19; N, 2.03; S, 18.46.

X-ray Crystallography. Diffraction intensities of the complexes were collected on a Bruker P4 diffractometer fitted with Mo-K radiation. The absorption correction was applied by using multiscan program SADABS.¹² The structures were solved with the direct method using SHELXTL¹³ and refined by a full-matrix least-squares refinement on F^2 with the SHELXL97.¹⁴ Anisotropic thermal parameters were applied to all non-hydrogen atoms and the hydrogen atoms placed in ideal positions. Crystal data as well as details of data collection and refinements for the complexes are summarized in Table 1.

Optical Measurements. The absorption spectra were recorded on a Shimadzu UV-2401PC spectrophotometer. To measure low-temperature luminescence and excitation spectra, samples in crystalline state were placed on the cold finger of a CTE-cryogenics refrigerator using silicon grease. Excited light from an Oriel 1000-W Xe arc lamp was passed through an Oriel MS257 monochromator and focused on the sample. The spectra were measured at an angle of 90 with an ARC

Table 1. Crystallographic data and refinement details for Pd(btnbmtmp)Cl₂ and Pt(btnbmtmp)Cl₂

Compound	Pd	Pt
Formula	$\text{C}_{23}\text{H}_{31}\text{Cl}_2\text{PdNS}_4$	$\text{C}_{23}\text{H}_{31}\text{Cl}_2\text{PtNS}_4$
Formula weight	627.03	715.72
Crystal system	monoclinic	monoclinic
Space group	$P2_1/n$	$P2_1/n$
a (Å)	14.7408(3)	14.6902(4)
b (Å)	10.9906(3)	11.0732(2)
c (Å)	17.4216(4)	17.4493(3)
β (°)	106.6820(10)	106.8670(10)
V (Å ³)	2703.69(11)	2716.33(10)
Z	4	4
D_{cal} (mg m ⁻³)	1.540	1.750
$F(000)$	1280	1408
μ (mm ⁻¹)	1.205	5.682
θ rang (°)	1.60 – 28.30	1.60 – 28.29
Reflections collected	27097	28013
/unique [$R(\text{int})$]	/6710 [0.0543]	/6718 [0.0447]
Completeness (%) [to θ (°)]	99.8 [28.30]	99.4 [28.29]
Data/restraints/parameters	6710/4/330	6718/4/330
Goodness-of-fit on F^2	0.994	1.016
$R1, \omega R2$ with $I \geq 2.0\sigma(I)$		
final	0.0456, 0.0780	0.0311, 0.0640
all data	0.1253, 0.1022	0.0492, 0.0706
Largest diff. peak and hole (e Å ⁻³)	0.706 -0.789	1.465 -0.805

0.5-m Czeny-Turner monochromator equipped with a cooled Hamamatsu R-933-14 photomultiplier tube. To measure solution-state spectra, all samples were dissolved in CH_2Cl_2 , and the concentrations were adjusted to approximately 10^{-3} – 10^{-4} M.

Results and Discussion

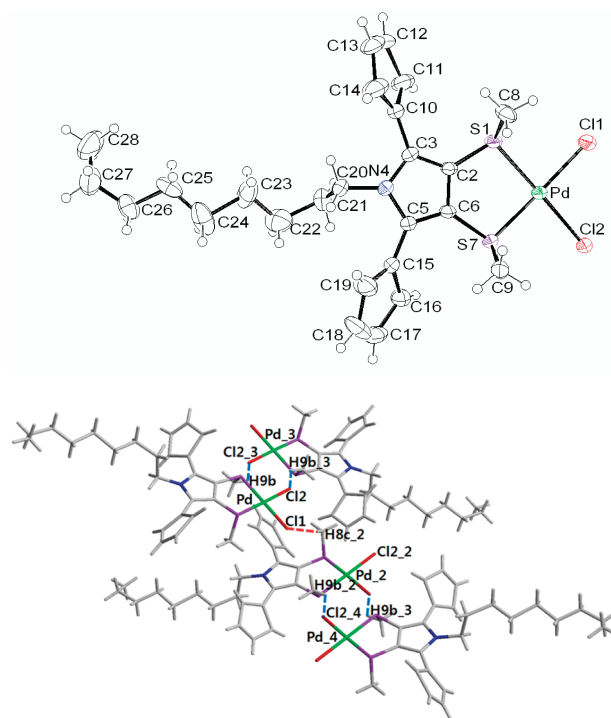
Crystal Structure. Both compounds Pd(btnbmtmp)Cl₂ and Pt(btnbmtmp)Cl₂ crystallized in the monoclinic $P2_1/n$ space group. Selected bond lengths and angles are listed in Table 2 and the asymmetric unit of Pd(btnbmtmp)Cl₂ is shown in Figure 1(a). The crystal structure of Pt(btnbmtmp)Cl₂ is very similar to that of Pd(btnbmtmp)Cl₂. The bond lengths and the bond angles of the four coordinate configuration of M(btnbmtmp)Cl₂ are very comparable to those of M(nbmtmp)Cl₂ (M = Pd and Pt).^{9,10} The sum of the bond angles of the four-coordinate metal ions are 359.95° for Pd and 360.30° for Pt. The root mean square (rms) deviation of the five atoms from the least-square's plane was 0.010 Å for both Pd(II) and Pt(II) complexes, indicating that the complexes formed a planar configuration around the metal ions. The average lengths of C–S bonds in two thiophene moieties are 1.638 Å for the Pd(II) complex and 1.639 Å for the Pt(II) complex. This average C–S bond length is markedly shorter than that of thiophene-benzobisthiazole (1.7273 Å).¹⁵ The two thiophene planes formed cis geometry to the pyrrole plane, and the angles of the two thiophene planes to the pyrrole plane are 58.44 and 51.22° for the Pd(II) complex and 60.50 and 50.87° for the Pt(II) complex. These dihedral angles between the thiophene and the pyrrole frames indicated that in

Table 2. Selected bond lengths (Å) and bond angles (°) of Pd-(btmbmp)Cl₂ and Pt(btmbmp)Cl₂

	Pd	Pt
M-S(1)	2.2747(11)	2.2591(9)
M-S(7)	2.2810(11)	2.2592(10)
M-Cl(2)	2.3123(11)	2.3186(9)
M-Cl(1)	2.3180(12)	2.3265(10)
S(1)-C(2)	1.752(4)	1.762(4)
S(1)-C(8)	1.798(4)	1.814(4)
C(3)-N(4)	1.376(5)	1.381(5)
N(4)-C(5)	1.380(5)	1.381(5)
N(4)-C(20)	1.473(5)	1.482(5)
C(6)-S(7)	1.754(4)	1.765(4)
S(7)-C(9)	1.796(4)	1.808(4)
C(10)-S(11)	1.667(5)	1.686(4)
S(11)-C(12)	1.636(5)	1.666(5)
C(15)-S(16)	1.655(5)	1.631(4)
S(16)-C(17)	1.592(6)	1.574(6)
S(1)-M-S(7)	92.07(4)	92.42(3)
S(1)-M-Cl(2)	178.22(5)	178.69(4)
S(7)-M-Cl(2)	86.71(4)	87.40(3)
S(1)-M-Cl(1)	86.44(4)	87.14(4)
S(7)-M-Cl(1)	177.64(4)	178.03(4)
Cl(2)-M-Cl(1)	94.73(4)	93.00(4)
C(2)-S(1)-C(8)	102.7(2)	102.56(18)
C(2)-S(1)-M	101.22(13)	101.44(12)
C(8)-S(1)-M	106.24(17)	107.20(15)
C(3)-N(4)-C(5)	109.6(3)	109.6(3)
C(3)-N(4)-C(20)	126.0(3)	124.9(3)
C(5)-N(4)-C(20)	123.5(3)	124.4(3)
C(6)-S(7)-C(9)	101.5(2)	101.04(19)
C(6)-S(7)-M	101.49(14)	101.76(13)
C(9)-S(7)-M	107.75(16)	108.33(14)

the near planar structure, the steric hindrances within the molecule became very energetically unfavorable. For M(btmbmp)Cl₂ (M = Pd and Pt), the isolated molecules were assembled to higher dimensional frameworks by forming a zig-zag S-H...Cl hydrogen-bonded with two adjacent molecules, as shown in Figure 1(bottom). For The H...Cl distance in the same direction (2.757 Å for Pd and 2.744 Å for Pt) is slightly shorter than that in the opposite direction (2.967 Å for Pd and 2.984 Å for Pt). Although the molecules included rich-electron heterocycles, no $\pi \cdots \pi$ stacking interaction was expected on the crystal structure formation because of the zig-zag crystal-network.

Optical Properties. Absorption: The absorption spectra of btmbmpH₂, and the Pd(II) and Pt(II) complexes dissolved in CH₂Cl₂ are shown in Figure 2, and the absorption data are summarized in Table 3. The Pd(II) complex produced three absorption bands, with peaks at 410.2, 313.2 and 244.7 nm (hereafter, referred to as A-, B- and C-absorption bands in order of increasing energy). The Pt(II) complex also produced the three absorption bands. Compared to those of the Pd(II) complex, the bands were slightly blueshifted and the A-band was very weak and appeared as a shoulder (see the spectrum inserted in Figure 2). The peak positions and the band shapes of the btmbmp complexes were very similar to the corresponding bands of the nbmtmp complexes. The only difference was

**Figure 1.** Perspective ORTEP drawing(top, thermal ellipsoids of 50%) and c-axis-projected packing diagram (bottom, symmetry equivalent positions : a; (x, y, z), b; (-x+1/2, y+1/2, -z+1/2), c; (-x, -y, -z), d; (x-1/2, -y-1/2, z-1/2) of Pd(btmbmp)Cl₂.**Table 3.** Electronic absorption data for btmbmpH₂, Pd(btmbmp)Cl₂ and Pt(btmbmp)Cl₂ dissolved in CH₂Cl₂

compound	Absorption band	$\epsilon / \text{M}^{-1}\text{cm}^{-1} (\lambda_{\text{abs}} / \text{nm})$
Free ligand	A-band	-
	B-band	$3.2 \times 10^4 (355.5)$
	C-band	$1.3 \times 10^5 (268.6)$
Pd complex	A-band	$2.4 \times 10^4 (410.2)$
	B-band	$1.2 \times 10^5 (313.2)$
	C-band	$4.6 \times 10^5 (244.7)$
Pt complex	A-band	$1.0 \times 10^3 (390.0)$
	B-band	$1.2 \times 10^5 (303.6)$
	C-band	$2.7 \times 10^5 (239.0)$

that the molar absorbance of the B- and C-absorption bands increased more than 10 times compared to those of the nbmtmp complexes. This was due to two substituted thiophene moieties. The $\pi \rightarrow \pi^*$ transitions of the thiophene moieties were reinforced to those of the pyrrole frame, accounting for as the B- and C-band absorptions. Specially, the relative intensity of the B-band to the C-band of the btmbmp complexes was strongly enhanced to produce the well-shaped B-band in the 280-350 nm region, which was observed as a weak band for the nbmtmp compounds. The A-absorption band associated with the $n \rightarrow \sigma^*$ transition of thiol was usually very weak but its oscillator strength increased to some extent by coordinating to the metal. Thiophene-benzobisthiazole dissolved in CH₂Cl₂ showed two characteristic absorption bands : a broad band ($\lambda_{\text{max}} = 362 \text{ nm}$, $\epsilon = 2.3 \times 10^4 \text{ M}^{-1} \text{ cm}^{-1}$) and a sharp band ($\lambda_{\text{max}} = 288 \text{ nm}$, $\epsilon = 1.9 \times 10^4 \text{ M}^{-1} \text{ cm}^{-1}$). The observed B-absorption band of

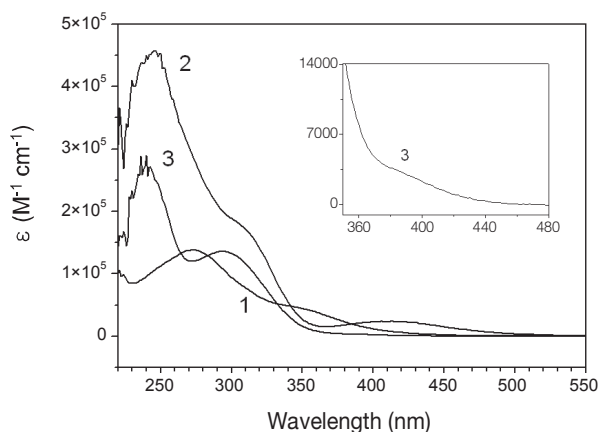


Figure 2. Absorption spectra of btbmptH₂ (1), Pd(btbmpt)Cl₂ (2) and Pt(btbmpt)Cl₂ (3) dissolved in CH₂Cl₂.

btbmptH₂ resembled the 362 nm band of thiophene-benzobisthiazole, conforming that the B-band is associated with the transitions of not only the pyrrole frame but also the thiophene moieties.

Luminescence and Excitation: Previously, we measured the luminescence and excitation spectra of the free ligand, nbmptH₂, dissolved in CH₂Cl₂. The nbmptH₂ solution exhibited two emission bands, peaking at 388 and 525 nm. The high- and low-energy emissions were mainly produced by the 320 and 403 nm excitations, respectively. These two excitations correspond to the B- and A-absorption bands of the nbmptH₂ ligand, respectively. The high- and low-energy emissions are associated with the $\pi \rightarrow \pi^*$ transition of the pyrrole frame and the $n \rightarrow \sigma^*$ transition of the thiol groups, respectively. Figure 3 shows the luminescence and excitation spectra of the btbmptH₂ ligand dissolved in CH₂Cl₂. In contrast to the case of nbmptH₂, the btbmptH₂ ligand produced only the low-energy emission, peaking at 530 nm. The emission from the pyrrole frame was completely quenched in the solution state. This may have been due to the interaction between the π electrons of the pyrrole frame and of the substituted thiophene moieties. As shown in Figure 3, the excitation and luminescence spectra are mirror image and the spectral range of the excitation corresponds to the low-energy shoulder, referred to as the A-absorption band. The peak position of the excitation

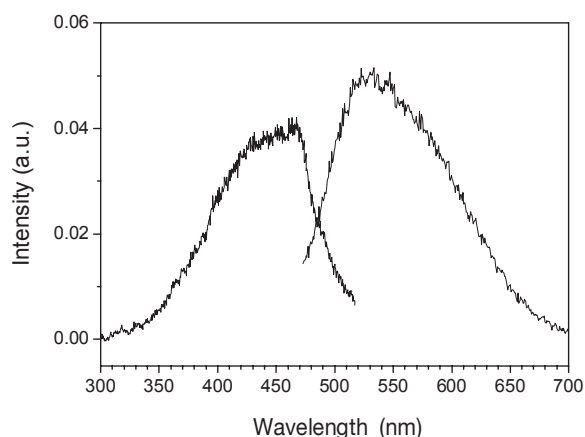


Figure 3. Luminescence ($\lambda_{\text{exn}} = 460$ nm) and excitation ($\lambda_{\text{ems}} = 560$ nm) spectra of btbmptH₂ dissolved in CH₂Cl₂.

band of the low-energy emission from btbmptH₂ was 450 nm, which was redshifted by about 50 nm compared to that of nbmptH₂. In the crystalline state, however, the ligand produced not only the low-energy emission but also the high-energy emission, as shown in Figure 4(a). The 325 nm He-Cd line excitation produced high-energy emission with relatively strong intensity at 400 nm and low-energy emission with relatively weak intensity in the 450-700 nm region. The low-energy emission composed of three Gaussian components, with peaks at 506, 537 and 577 nm. The multi-peak structure was due to the vibronic distortion, which is usually observed in thiols. The A-band excitation ($\lambda_{\text{exn}} = 460$ nm) also produced low-energy emission with multi-peak structure, as shown in Figure 4(b). The excitation spectrum of the low-energy emission is very broad, spanning over the 330-500 nm region with the peak position at 470 nm, as shown in Figure 4(c). Compared to the solution state, the emission and excitation spectra of the crystals were redshifted as usual. The excitation spectrum of the high-energy emission with a peak at 350 nm spanned over the 250-370 nm region and was the mirror-image of the high-energy emission band. This indicated that the high-energy emission was responsible for emission from the pyrrole frame, which did not appear in the solution state.

The complex of Pd(btbmpt)Cl₂ dissolved in CH₂Cl₂ produced no luminescence, and its luminescence intensity

Table 4. Excitation and emission data* and assignment of emissive transitions for btbmptH₂, Pd(btbmpt)Cl₂ and Pt(btbmpt)Cl₂

	Excitation (nm)	Emission (nm)	Assignment
btbmptH ₂ (CH ₂ Cl ₂) (solid)	450 350 470	530 405 506(p), 537(p), 577(s)	$\sigma^* \rightarrow n$ (S, thiol) $\pi^* \rightarrow \pi$ (pyrrole) $\sigma^* \rightarrow n$ (S, thiol)
Pd(btbmpt)Cl ₂ (solid)	325-nm HeCd line	396 587	$\pi^* \rightarrow \pi$ (pyrrole) $\sigma^* \rightarrow n$ (S, thiol)
Pt(btbmpt)Cl ₂ (solid)	350 420 440	530 - 720	d (Pt) \rightarrow n (S, thiol) $\sigma^* \rightarrow n$ (S, thiol) p (Pt) \rightarrow n (S, thiol)

* The data for the solid state was obtained at 70 K.

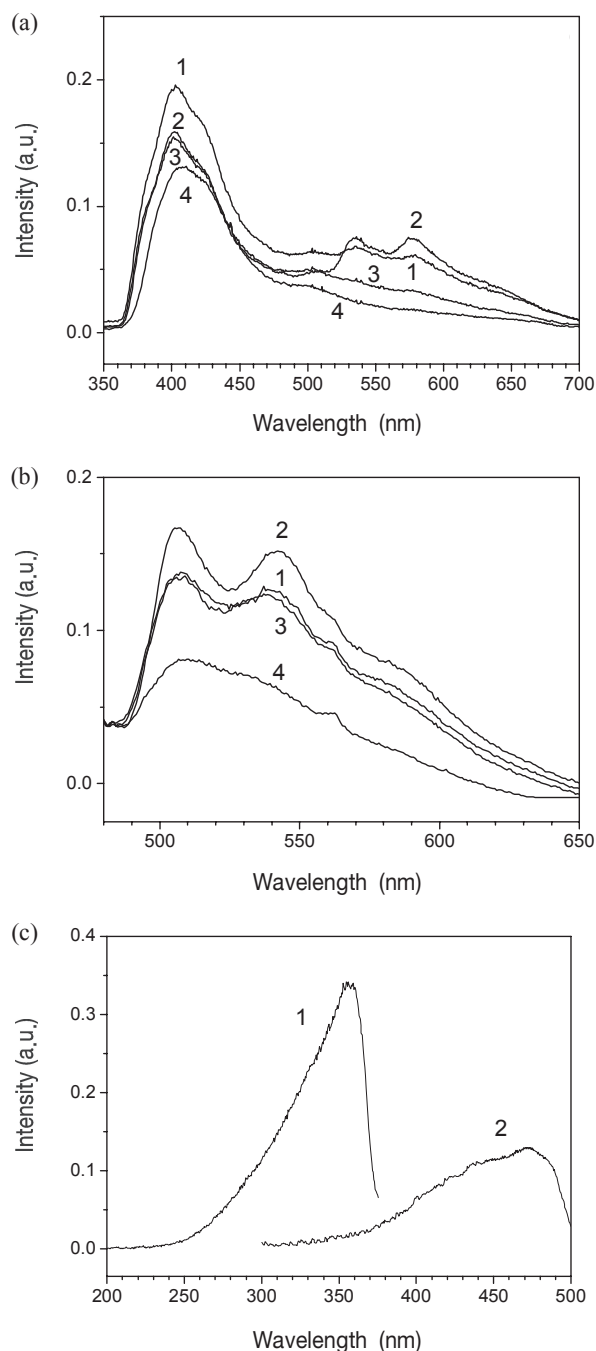


Figure 4. (a) PL and (b) luminescence ($\lambda_{\text{exn}} = 460$ nm) spectra of btbmbtpH₂ in crystalline state, measured at various temperatures ($T = 1; 10$ K, 2; 70 K, 3; 150 K, 4; RT), and (c) excitation spectra ($\lambda_{\text{ems}} = 1; 405$ nm, 2; 533 nm) at $T = 10$ K.

was very weak even in the crystalline state. Figure 5(a) shows the PL spectra of the crystals, measured at various temperatures. At room temperature, the complex produced only background intensity. At low temperature, the crystals produced the high- and low-energy emissions spanning over the 350–700 nm region. The PL intensity of the complex at low temperature was much weaker (approximately 50 times) than that of the ligand. The spectral shape of the high-energy emission, however, was very similar to that of the ligand. Although the low-energy emission appeared in the longer

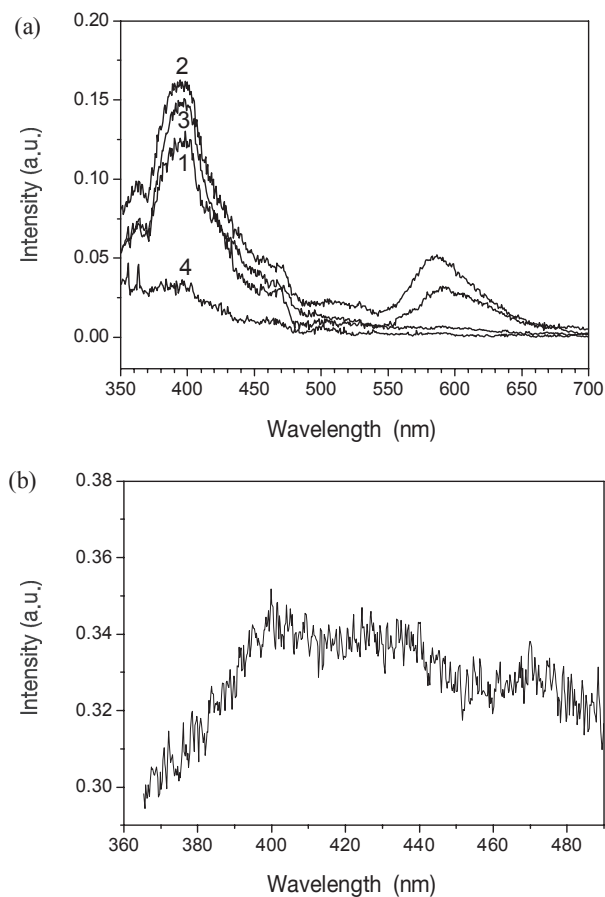


Figure 5. PL and excitation spectra of Pd(btnbmtpt)Cl₂ in crystalline state: (a) PL measured at 1; 10 K, 2; 70 K, 3; 150 K and 4; RT ($\lambda_{\text{exn}} = 325$ nm He–Cd line) and (b) excitation measured at 10 K ($\lambda_{\text{ems}} = 620$ nm).

wavelength region compared to that of the ligand, the excitation spectrum of the 580 nm emission measured at $T = 70$ K was very similar to that from the ligand, as shown in Figure 5(b).

The Pt(II) complex in solution and crystalline states produced no luminescence at room temperature. In crystalline state, however, the 325 nm excitation produced only the low-energy emission spanning over the 520–750 nm region, as shown in Figure 6(a). The PL intensity was very strong (more than 10 times) compared to that of the ligand. As shown in Figure 6(b) and (c), the A- and B-band excitations produced broad luminescence from yellow to deep red. This spectral range was markedly redshifted compared to the low-energy emission (green-orange) from the thio moieties of the ligand. The spectral shape of the A-band emission ($\lambda_{\text{exn}} = 340$ nm) was somewhat different from that of the B-band emission ($\lambda_{\text{exn}} = 420$ nm). The A-band emissions composed of three Gaussian components, with peaks at 562, 624 and 680 nm. The intensities of the two low-energy components were enhanced by the A-band excitation. The excitation spectra were measured at 70 K by monitoring four different emissions. As shown in Figure 6(d), the spectral features of the excitation were somewhat dependent on the observed emission wavelength. For the 560 nm emission, the excitation spectrum was composed of two bands, with peaks at 350 and 440 nm. The 440 nm excitation band was almost the same as that of the ligand,

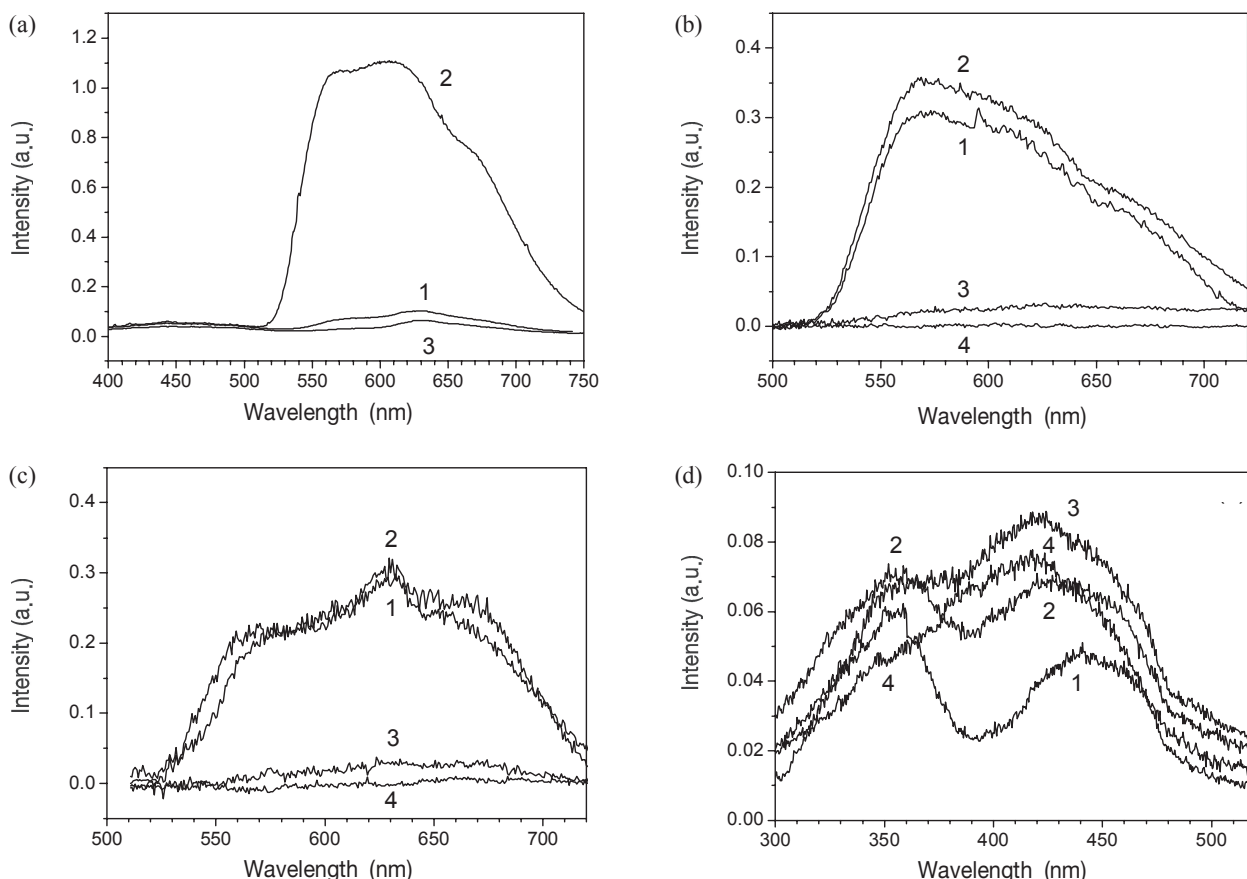


Figure 6. (a) PL and (b,c) luminescence ($\lambda_{\text{exc}} =$: b; 340 nm, c; 420 nm) spectra of Pt(btnbmtmp)Cl₂, measured at various temperatures ($T =$: 1; 10 K, 2; 70 K, 3; 150 K, 4; RT), and (d) excitation spectra ($\lambda_{\text{ems}} =$: 1; 560 nm, 2; 600 nm, 3; 640 nm, 4; 680 nm) at $T = 10$ K.

which was attributed to the $n \rightarrow \sigma^*$ transition of the thio moieties. It is unlikely that the nature of the 350 nm excitation band is absolutely different from that of the free ligand in the crystalline state. For the ligand in the crystalline state, excitation at 350 nm produced emission at 403 nm with a narrow bandwidth, which originated from the $^1(\pi\pi^*)$ excited state of the pyrrole frame, while for the Pt(II) complex, excitation at 350 nm produced broad emission from yellow to deep red. A possible model for the 350 nm excitation is the charge transfer transition from the nonbonding orbital of S to a high-lying orbital of Pt(II). The peak position of the high-energy excitation band was almost independent of the monitoring emission wavelength up to $\lambda_{\text{ems}} = 640$ nm. With increasing monitoring emission wavelength, however, the peak position of the low-energy excitation band was blueshifted and its relative intensity increased. For $\lambda_{\text{ems}} = 680$ nm, the excitation spectrum showed one peak at 420 nm. For Pt(nbmtmp)Cl₂, the single crystals were found to produce a red emission, with a peak at 625 nm *via* the charge transfer from S to Pt. The charge-transfer excitation spectrum extended over the region from 300 to 480 nm with a peak at 420 nm. The similarity suggested that the 420 nm excitation could be associated with the charge transfer transition from the nonbonding orbital of the thio moieties to a low-lying orbital of Pt(II).

To clarify the observed luminescence properties of Pt(btnbmtmp)Cl₂, a quantum mechanical calculation was performed using SDD basis functions (LanL2DZ for Pt; 6-31G(d) for S

and Cl; 6-31G for the rest atoms). As in the case of the Pt(nbmtmp)Cl₂ molecule, the main component of the lowest unoccupied molecular orbital (LUMO) is $d_{x^2-y^2}$ of Pt, forming a σ^* orbital with S and Cl, by taking the square-plane molecular axes along the x- and y-axes under the C_{2v} symmetry. The next several LUMOs were made from the π^* orbitals of the thiophene moieties and/or the s and p orbitals of Pt. Among LUMOs contributed mainly from the Pt orbitals, the order of the energy level was $\text{LUMO}(p_z) < \text{LUMO}(p_x) \leq \text{LUMO}(p_y) < \text{LUMO}(s)$. Accordingly, the 420 nm and 350 nm excitations can be attributed to the transitions from the nonbonding orbitals of the thio moieties to the $d_{x^2-y^2}$ and p_z orbitals of Pt, respectively.

Conclusion

The substitution of thiophenes at the 2 and 5 positions of the 3,4-bis(methylthio)pyrrole derivative, nbmptH₂, was very unfavorable for the luminescence properties of the free ligand and its metal complexes. In the CH₂Cl₂ solution, the unsubstituted nbmptH₂ and its metal complexes excited with UV light produced two emission bands: emission at 402 nm from the pyrrole frame and emission at 525 nm from the thiol moieties. For 2,5-dithiophene substituted btnbmtptH₂, the emission from the pyrrole frame of the free ligand and its Pd(II) and Pt(II) complexes was almost quenched in the solution. Furthermore, the emission originated from the charge

transfer from S to Pt(II), which was unique for Pt(nbmpt)Cl₂ in crystalline state. For Pt(btnbmpt)Cl₂, however, the crystals excited by UV light produced the yellow to deep-red emission with lowered intensity *via* direct excitation of the thio groups and the charge transfer to Pt(II). These unfavorable results could have been due to the π -electron interaction between the pyrrole frame and the thiophen moieties lying with the average dihedral angle of 55.26°.

Acknowledgments. This research was partly supported by Kumho Electric Inc. and by a research grant of Kwangwoon University (2008). J.-G. K. and S.-I. O. acknowledge the fellowships of the BK 21 program.

Supplementary Materials. Supplementary data associated with this article can be obtained free of charge from the Cambridge Crystallographic Data Centre (CCDC 719048 for Pd(btnbmtp)Cl₂ and CCDC 719049 for Pt(btnbmtp)Cl₂).

References

- (a) Nielsen, C. B.; Angerhofer, A.; Abboud, K. A.; Reynolds, J. R. *J. Am. Chem. Soc.* **2008**, *130*, 9734; (b) Ma, C.; Taya, M.; Xu, C. *Electrochim. Acta* **2008**, *54*, 598.
- (a) Johansson, T.; Mammo, W.; Svensson, M.; Andersson, M. R.; Inganäs, O. *Chem. Mater.* **1999**, *11*, 3133; (b) Egbe, D. A. M.; Nguyen, L. H.; Muehlbacher, D.; Hoppe, H.; Schmidtke, K.; Sariciftci, N. S. *Thin Solid Films* **2006**, *511*, 486; (c) Zhou, E.; Tan, Z.; Huo, L.; He, Y.; Yang, C.; Li, Y. *J. Phys. Chem. B* **2006**, *110*, 26062; (d) Sergawie, A.; Admassie, S.; Mammo, W.; Yohannes, T.; Solomon, T. *Syn. Metals* **2008**, *158*, 307; (e) Li, G.; Jiang, K.-J.; Li, Y.-F.; Li, S.-L.; Yang, L.-M. *J. Phys. Chem. C* **2008**, *112*, 11591.
- (a) Brabec, C. J.; Winder, C.; Sariciftci, N. S.; Hummelen, J. C.; Dhanabalan, A.; Van Hal, P. A.; Janssen, R. A. J. *Adv. Funct. Mater.* **2002**, *12*, 709; (b) Hissler, M.; Lescop, C.; Reau, R. *Pure Appl. Chem.* **2005**, *77*, 2099; (c) Kuo, W.-J.; Chen, Y.-H.; Jeng, R.-J.; Chan, L.-H.; Lin, W.-P.; Yang, Z.-M. *Tetrahedron* **2007**, *63*, 7086; (d) Wu, S.-H.; Huang, H.-M.; Chen, K.-C.; Hu, C.-W.; Hsu, C.-C.; Tsiang, R. C.-C. *Adv. Funct. Mater.* **2006**, *16*, 1959; (e) Hobbs, M. G.; Baumgartner, T. *Eur. J. Inorg. Chem.* **2007**, 3611; (f) Kuila, B. K.; Garai, A.; Nandi, A. K. *Chem. Mater.* **2007**, *19*, 5443; (g) Cheylan, S.; Bolink, H. J.; Fraleoni-Morgera, A.; Puigdollers, J.; Voz, C.; Mencarelli, I.; Setti, L.; Alcubilla, R.; Badenes, G. *Org. Electronics* **2007**, *8*, 641; (h) Qi, Z.-J.; Feng, W.-D.; Sun, Y.-M.; Yan, D.-Z.; He, Y.-F.; Yu, J. *J. Mater. Sci.: Mater. Electronics* **2007**, *18*, 869; (i) Matsushima, T.; Adachi, C. *Chem. Mater.* **2008**, *20*, 2881.
- (a) Zhou, Q.; Li, C. M.; Li, J.; Cui, X.; Gervasio, D. *J. Phys. Chem. C* **2007**, *111*, 11216; (b) Henderson, J. C.; Kiya, Y.; Hutchison, G. R.; Abruna, H. D. *J. Phys. Chem. C* **2008**, *112*, 3989; (c) Rudge, A.; Raistrick, I.; Gottesfeld, S.; Ferraris, J. P. *Electrochim. Acta* **1994**, *39*, 273; (d) Henderson, J. C.; Kiya, Y.; Hutchison, G. R.; Abruna, H. D. *J. Phys. Chem. C* **2008**, *112*, 3989.
- Guernion, N. J. L.; Hayes, W. *Curr. Org. Chem.* **2004**, *8*, 637.
- Li, H.; Lambert, C.; Stahl, R. *Macromol.* **2006**, *39*, 2049.
- Goldoni, F.; Antolini, L.; Pourtois, G.; Schenning, A. P. H. J.; Janssen, R. A. J.; Lazzaroni, R.; Brédas, J.-L.; Meijer, E. W. *Eur. J. Inorg. Chem.* **2001**, 821.
- Matthews, J. R.; Goldoni, F.; Kooijman, H.; Spek, A. L.; Schenning, A. P. H. J.; Meijer, E. W. *Macromol. Rapid Comm.* **2007**, *28*, 1809.
- Kang, J.-G.; Cho, D.-H.; Park, C.; Kang, S. K.; Kim, I. T.; Lee, S. W.; Lee, H. H.; Lee, Y. N.; Lim, D. W.; Lee, S. J.; Kim, S. H.; Bae, Y. J. *Bull. Korean Chem. Soc.* **2008**, *29*, 599.
- Kang, J.-G.; Cho, H.-K.; Park, C.; Kang, S. K.; Kim, I. T.; Lee, S. W.; Lee, H. H.; Lee, Y. N.; Cho, S. H.; Lee, J. H.; Lee, S. H. *Bull. Korean Chem. Soc.* **2008**, *29*, 679.
- Richards, J. J.; Melander, C. J. *Org. Chem.* **2008**, *73*, 5191.
- Sheldrick, G. M. *Program SADABS; Area-detector absorption correction* University of Göttingen: Göttingen, Germany, 1996.
- SHELXTL*, 5.030 ed.; Bruker Analytical X-ray Instruments, Inc.: Madison, WI, 1998.
- Sheldrick, G. M. *SHELXS-97, SHELXL-97, Programs for Crystal Structure Analysis*; University of Göttingen: Göttingen, Germany, 1997.
- Kang, J.-G.; Cho, H.-G.; Kang, S. K.; Park, C.; Lee, S. W.; Park, G. B.; Lee, J. S.; Kim, I. T. *J. Photochem. Photobio. A: Chem.* **2006**, *183*, 212.